

| REPORT DOCUMENTATION PAGE  |  |   | Form Approved<br>OMB No. 0704-0188      |  |
|--|--|---|---|--|
| <small>Public reporting burden for this collection of information is estimated to average 1 hour per response, including the time for reviewing instructions, searching existing data sources, gathering and maintaining the data needed, and completing and reviewing the collection of information. Send comments regarding this burden estimate or any other aspect of this collection of information, including suggestions for reducing this burden, to Washington Headquarters Services, Directorate for Information Operations and Reports, 1215 Jefferson Davis Highway, Suite 1204, Arlington, VA 22202-4302, and to the Office of Management and Budget, Paperwork Reduction Project (0704-0188), Washington, DC 20503.</small>  |  |   |   |  |
| 1. AGENCY USE ONLY (Leave blank)   | 2. REPORT DATE<br>December 12, 1995                      | 3. REPORT TYPE AND DATES COVERED<br>Final - SEP-93-SEP '95  |   |  |
| 4. TITLE AND SUBTITLE<br>Equipment for Enhancing and Extending Fluid Mechanics and Heat Transfer Research in Aeroengines   |  | 5. FUNDING NUMBERS<br>DEPSCOR Equipment Grant<br>No. F49620-93-1  |   |  |
| 6. AUTHOR(S)<br>Ting Wang and Mark Pinson  |  | 0533  |   |  |
| 7. PERFORMING ORGANIZATION NAME(S) AND ADDRESS(ES)<br>Department of Mechanical Engineering<br>Clemson University<br>Clemson, SC 29634-0921   |  | 8. PERFORMING ORGANIZATION REPORT NUMBER<br>AFOSR-TR-96-0014  |   |  |
| 9. SPONSORING/MONITORING AGENCY NAME(S) AND ADDRESS(ES)<br>Dr. James M. McMichael<br>Air Force Office of Scientific Research<br>AFOSR/NA<br>Bolling AFB, DC 20332-6448   |  | 10. SPONSORING/MONITORING AGENCY REPORT NUMBER<br>F49620-93-1-0533  |   |  |
| 11. SUPPLEMENTARY NOTES<br>This equipment grant has supported the projects funded by AFOSR Grant No. F49620-94-0126 and by DoD EPSCoR Fellowship Grant No. F49620-92-J-0459  |  |   |   |  |
| 12a. DISTRIBUTION / AVAILABILITY STATEMENT<br>Approved for public release,<br>distribution unlimited   |  | 12b. DISTRIBUTION CODE<br>DISTRIBUTION STATEMENT A<br>Approved for public release<br>Distribution Unlimited |   |  |
| 13. ABSTRACT (Maximum 200 words)<br><br>The DoD Grant (No. F49620-93-1) has been used to significantly expand and upgrade the capabilities of the facilities and instrumentation used by projects supported by AFOSR Grant No. F49620-94-0126 and by DoD EPSCoR fellowship grant No. F49620-92-J-0459. These two projects focus on experimental studies for flow and thermal structures in the hot flow passage in gas turbines. A summary of the expenditures has been included. Some changes were made from the original budget, and the details of these changes have been provided. Several custom-manufactured probes were specifically designed for measuring heat transfer and fluid flow structures within transitional boundary layers. The preliminary results were able to resolve the controversial issue regarding the negative value of cross-stream Reynolds heat flux ( $\overline{vT}$ ) in a transitional boundary layer. The expanded capability of the instrumentation also benefited research on the Advanced Turbine Systems project sponsored by the Department of Energy and on heat transfer enhancement using micro-structured surfaces sponsored by the 3M Company. |  |   |   |  |
| 14. SUBJECT TERMS<br>Hot Wire Sensors, Vorticity Probe, Reynolds Heat Flux   |  | 15. NUMBER OF PAGES<br>35   |   |  |
|  |  | 16. PRICE CODE  |   |  |
| 17. SECURITY CLASSIFICATION OF REPORT<br>Unclassified  | 18. SECURITY CLASSIFICATION OF THIS PAGE<br>Unclassified | 19. SECURITY CLASSIFICATION OF ABSTRACT<br>Unclassified   | 20. LIMITATION OF ABSTRACT<br>Unlimited |  |

19960228 111

## TABLE OF CONTENTS

|  |    |
|--|----|
| ABSTRACT                               | 1  |
| EXPENDITURES                           | 2  |
| JUSTIFICATION OF CHANGES               | 4  |
| NEW TEST SECTION                       | 7  |
| DATA ACQUISITION AND PROCESSING SYSTEM | 12 |
| PROBE DESIGNS AND PRELIMINARY RESULTS  | 14 |
| CURRENT STATUS                         | 28 |
| PUBLICATIONS                           | 29 |
| PERSONNEL                              | 30 |
| APPENDIX                               | 31 |

## ABSTRACT

The DoD Grant (No. F49620-93-1) has been used to significantly expand and upgrade the capabilities of the facilities and instrumentation used by projects supported by AFOSR Grant No. F49620-94-0126 and by DoD EPSCoR fellowship grant No. F49620-92-J-0459. These two projects focus on experimental studies for flow and thermal structures in the hot flow passage in gas turbines. A summary of the expenditures has been included. Some changes were made from the original budget, and the details of these changes have been provided. Several custom-manufactured probes were specifically designed for measuring heat transfer and fluid flow structures within transitional boundary layers. The preliminary results were able to resolve the controversial issue regarding the negative value of cross-stream Reynolds heat flux ( $\overline{v_t}$ ) in a transitional boundary layer. The expanded capability of the instrumentation also benefited research on the Advanced Turbine Systems project sponsored by the Department of Energy and on heat transfer enhancement using micro-structured surfaces sponsored by the 3M Company.

## EXPENDITURES

A summary of the expenditures is provided below in Table 1. Note that the entries with asterisk(s) denote changes or modifications from the original budget. Two significant additions to the budget are the "New Test Section" and the "48-Channel Pressure Scanner". These items were added to the budget on 18 October 1994, and they were approved on 5 January 1995 (See Appendix for copies of these communications). For reference the original budget is provided in Table 2.

Table 1. Summary of Expenditures

|   |               |
|---|---------------|
| Sensor a: (3-Wire B)  | \$ 5,077.00   |
| Sensor b: (3-Wire C and 3-Wire D)                             | \$ 3,215.38   |
| Sensor c: (Vorticity Sensor and 6-Wire Rake)                  | \$ 6,100.50   |
| Laser Printer: HP LaserJet 4M                                 | \$ 1,880.55   |
| Personal Computer   | \$ 3,590.28   |
| Workstation   | \$ 26,063.38  |
| SparcStation 10, Model 51                                     |               |
| 10.8 GB External HD Capacity***                               |               |
| Software  |               |
| Macintosh   | \$ 6,171.23   |
| Quadra 660AV  |               |
| 20 MB RAM***  |               |
| 730 MB HD Capacity***   |               |
| Software and accessories                                      |               |
| Ten 10-channel Fluke thermocouple modules                     | \$ 4,787.97   |
| Three-channel TSI IFA-100 hot-wire anemometer system***       | \$ 17,690.70  |
| Two-channel "PC real-time oscilloscope"*                      | \$ 5,732.01   |
| New Test Section**  | \$ 13,484.95  |
| Eight-channel, 16-Bit data acquisition system and accessories | \$ 9,014.25   |
| 48-Channel pressure scanner**                                 | \$ 3,410.96   |
| Misc. Laboratory Equipment***                                 | \$ 3,532.37   |
| Voltmeter w/ accessories                                      |               |
| probe support   |               |
| power controller  |               |
| TOTAL:  | \$ 109,751.53 |

\*Changes from original budget (see next section for explanation)

\*\*Approved changes to original budget

\*\*\*Expanded capability resulting from (\*) and (\*\*) items

Table 2. Original Budget

|   |           |
|---|-----------|
| Sensor a :  | \$5,000   |
| Sensor b :  | \$5,000   |
| Sensor c :  | \$6,500   |
| Laser Printer: HP LaserJet 4M   | \$2,060   |
| Personal computer:<br>486-66 Mhz, 1 GB hard disk, 64 MB RAM, and accessories.   | \$5,840   |
| Workstation:<br>Sparc Station 10 Model 41 with C++ and FORTRAN compilers,<br>signal analysis package, and 3 GB external hard drive. | \$25,890  |
| Macintosh:<br>Centris 650, 8 MB RAM, 230 MB hard drive, software,<br>and accessories.   | \$ 7,750  |
| Ten 10-channel Fluke thermocouple modules   | \$6,700   |
| Two-channel TSI IFA 100 hot-wire anemometer system  | \$14,900  |
| Two-channel Nicolet Pro 10 digital storage oscilloscope<br>and accessories  | \$16,175  |
| Eight-channel, 16-bit data acquisition boards and accessories   | \$8,109   |
| Equipment Total   | \$103,924 |
| 5% South Carolina State Tax   | \$5,196   |
| Estimated Shipping Expenses   | \$ 500    |
| TOTAL   | \$109,620 |

JUSTIFICATION OF CHANGES  
(Approved by AFOSR 5 January 1995)

Two-channel "PC real-time oscilloscope"

A stand-alone, real-time digital storage oscilloscope was called for under the original budget. With an estimated cost of \$16,175, the system was to provide the operator with detailed information regarding the steadiness of the overall flow situation and the heat transfer behavior during the course of each test run. Upon further investigation of available systems, it was found that this type of stand-alone device is generally difficult to use due to the rather obscure user interface that the operator has to work with. In addition, the analysis capabilities (i.e. the robustness of the functions that may be applied to the incoming signals) were limited. In many cases, the operator only has the capability to obtain a Fourier transform of the data. For the purposes of the tests to be conducted, this limited analysis capability was unacceptable.

An alternative to the stand-alone digital oscilloscope was found in the form of a PC data acquisition card with associated software from National Instruments Corporation. The data acquisition card is capable of acquiring data with 16-bit resolution at a maximum sample rate of 44 kHz for two channels. The system can store acquired data in a local memory buffer to allow subsequent analysis by an on-board DSP chip. The software purchased with the card includes all the data reduction routines necessary for detailed analysis of the signal. These routines have been optimized for use with the DSP chip so that the software/hardware combination provides performance close to that available from the stand-alone oscilloscope systems. Since the software package in the "PC oscilloscope" system is user defined, the operator can program a user interface that is most appropriate for the given application; therefore, operating efficiency during experimental testing is maximized.

Although the "PC oscilloscope" system requires a computer, a computer (purchased previously using parent program funds) was available. This system is completely separate from the computer system used to acquire data during experimental testing so it will not be necessary to interrupt data acquisition to use the "PC oscilloscope" system to check the flow/heat transfer conditions. An added benefit is that the data acquired by the system is already on a standard PC platform which allows the results to be downloaded much more easily than would be possible using the proprietary interface of a stand-alone oscilloscope. The National Instruments hardware/software was purchased for \$5,732.01, which provided a much more robust analysis platform at only 35% of the original cost projection.

## New Test Section

The original budget did not allow for the replacement of an existing test section; however, a year after the budget was approved and after expenditures were initiated, it was discovered that the existing test section had deteriorated at a faster pace than expected after 5 years' usage. Therefore, a request to replace the test section was submitted in October 1994 for the following reasons:

1. One of the primary reasons that the existing facility was replaced was because of problems within the heated test surface. The original heater design was a layered design that was assembled on-site. Long-term usage resulted in the separation of some of these layers. These gaps introduced a large degree of uncertainty into the heat transfer measurements.
2. The existing test section only allowed boundary layer measurement probes to be inserted through discrete access ports. The arrangement of these access ports did not allow for continuous adjustment of the measurement locations which is necessary to obtain detailed boundary layer growth information. As a result, the regions between the measurement ports were not accessible for some important measurements.
3. The old section only allowed for a single test surface (the aforementioned layered heated test surface). A different test surface could be placed into the flow only if the entire test section were replaced with another one.
4. The overall flow condition of the section was constrained to be either constant-speed flow, accelerated flow, or decelerated flow. Combinations of acceleration and deceleration could not easily be achieved.

For these reasons, a new test section was designed and constructed using this equipment fund. The next section of this report provides the details of the new design.

## 48-Channel Pressure Scanner

A 48-channel pressure scanning system was purchased for use with the new test section in order to further extend the capabilities of the laboratory. One of the focus points in the parent program is the study of separated boundary layer flow. To aid in the identification and localization of the separated flow phenomenon, a second unheated test surface was designed with 48 pressure taps placed at strategic locations along the surface. The new test section has been designed to facilitate multiple

test surfaces, and the pressure scanner system automates acquisition of the instantaneous pressure signals from each of the pressure ports during experimental testing.



## NEW TEST SECTION

An overview of the test facility is shown in Figure 1. The flow moves from left to right in Figure 1. A fan pulls air through a filter and then pushes it through a heat exchanger, a screen pack, and into the new test section. The test section is comprised of three parts: the frame, the "outer wall", and the test surface. The diagram of the frame shown in Figure 2 is shown without the outer wall or the test surface in place. The frame was designed to facilitate removal of both the outer wall and the test surface. When the outer wall and the test surface are fitted into the frame as shown in Figure 3, a confined flow area is formed. The outer wall is a thin Plexiglas sheet with a series of slots cut into it to allow probe access to the flow. The sheet is thin enough that it may be bent into the flow area or moved away to accelerate or decelerate the flow, respectively. Currently, two test surfaces have been constructed for use with the frame/outer wall assembly.

One of the test surfaces is a heated surface that has a series of thermocouples and a heater embedded beneath the surface. Figure 4 shows the locations of the 184 E-Type thermocouples placed along the surface, and Figure 5 documents the different layers of the heated test surface. At its lowest level, a layer of Lexan provides structural support for the heater and thermocouples. The upper portions of the test surface contain the thermocouples and a series of monel strips which are the elements forming the heater. The size and layout of these metal strips are shown in Figure 6. The previous heated surface was of a similar layered design; however, the layers of the old heater were assembled on-site with room temperature adhesives. When this old design was subjected to the desired operating conditions, the adhesives holding the layers together gradually deteriorated. To prevent the layers of the new heated surface from separating, Electrofilm (the heater manufacturer) laid out the monel element and the thermocouples in a epoxy board sandwich. The entire unit was cured at elevated temperatures to allow the epoxy board to soften and mold itself around both the heater and the thermocouples. At the conclusion of the curing process, the layers of epoxy formed a single cohesive unit containing the thermocouples and the heating elements.

The second surface is unheated and contains a series of pressure ports to facilitate measurement of local pressure fluctuations during experimental testing. The locations of these pressure ports are shown in Figure 7. A total of 48 pressure ports were placed along the surface, and use of the 48-channel pressure scanner will allow automated monitoring of the pressures during testing.

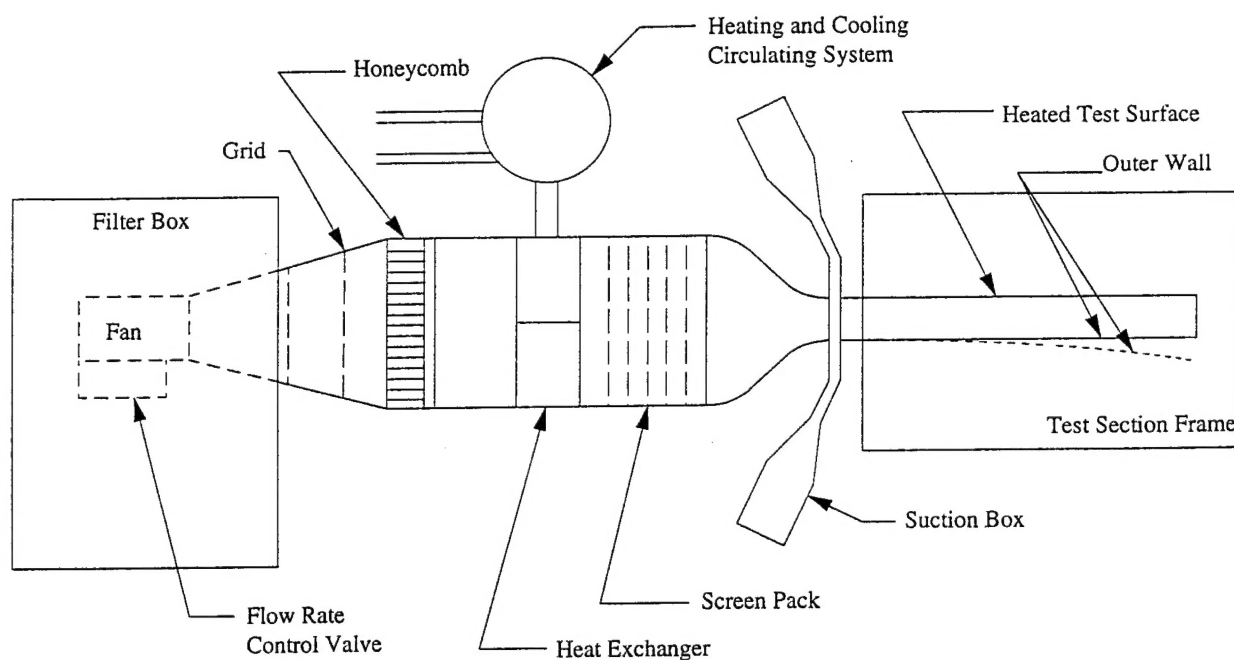


Figure 1. Overview of Low-Speed Two-Dimensional Boundary Layer Wind Tunnel Facility

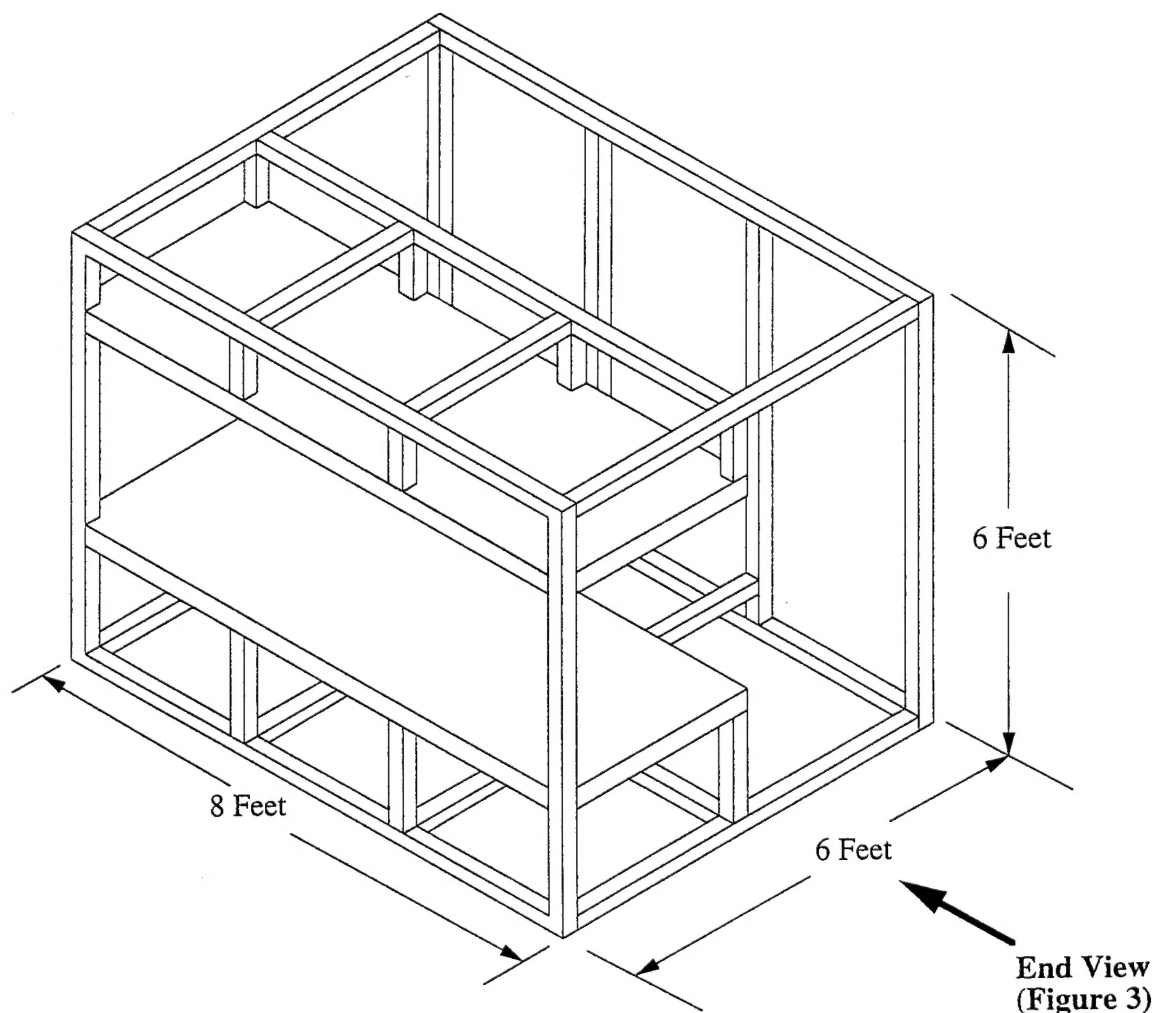


Figure 2. Overview of Test Section Frame

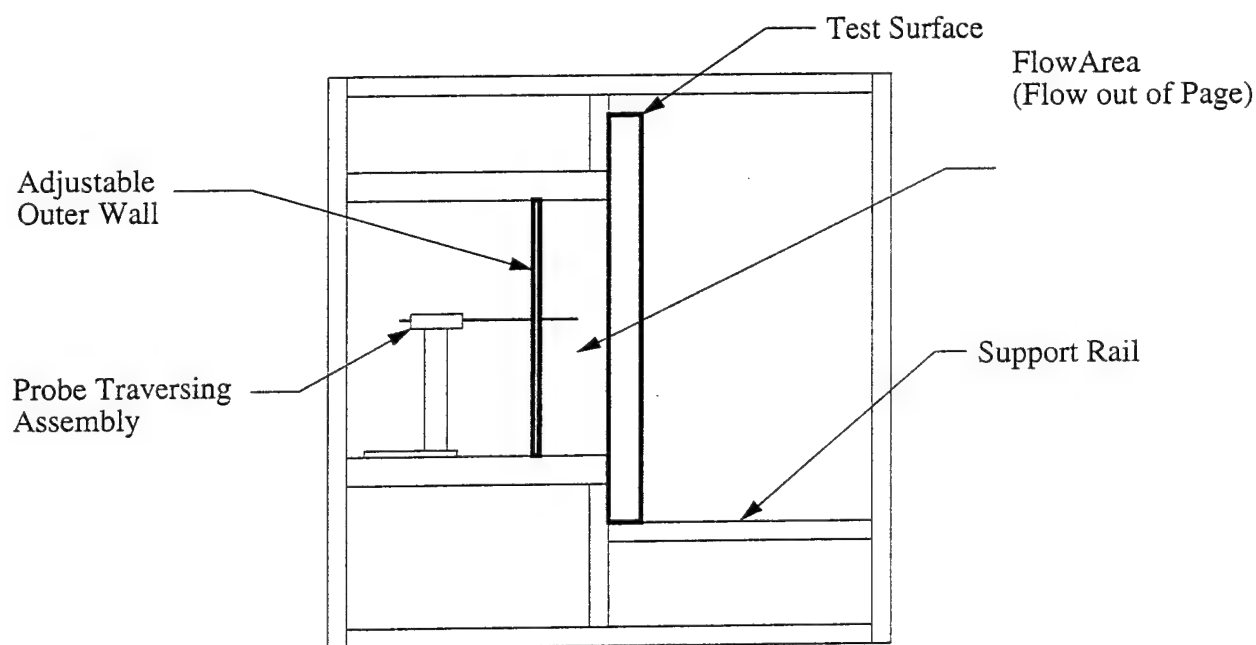


Figure 3. End View of Test Section

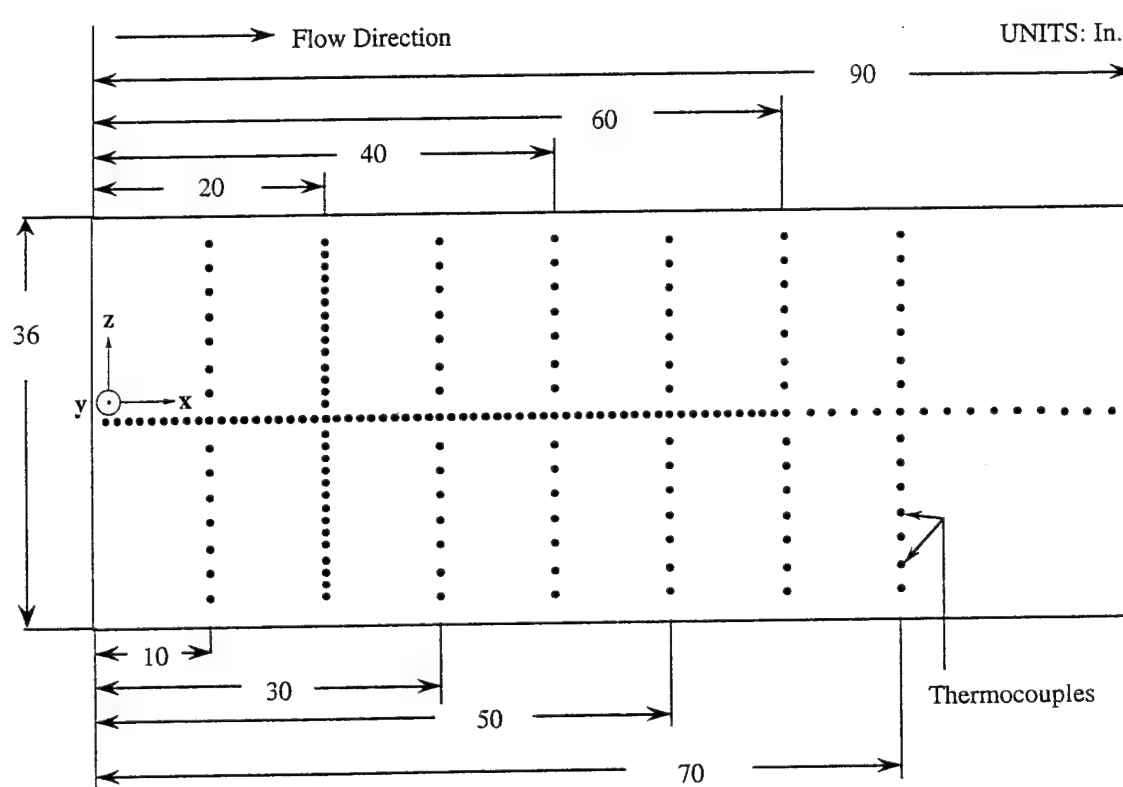


Figure 4. Schematic Diagram of the Thermocouple Locations on the Heated Test Surface

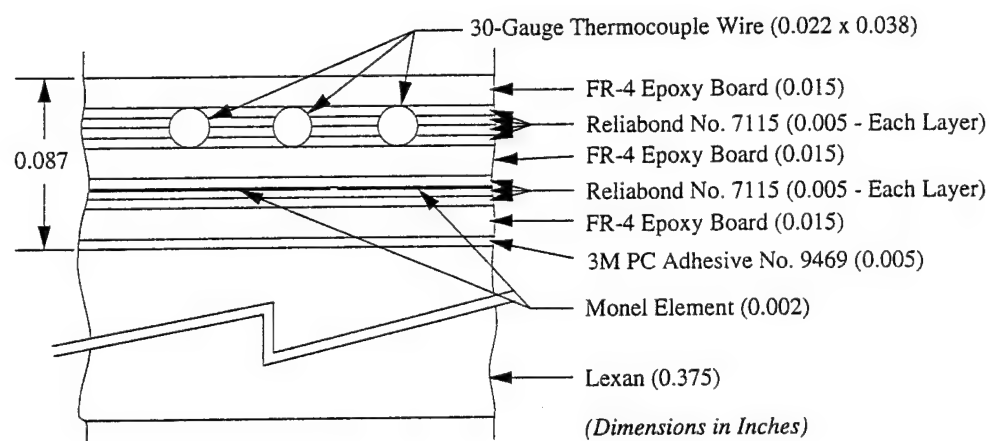


Figure 5. Cross-Section of Heated Test Surface

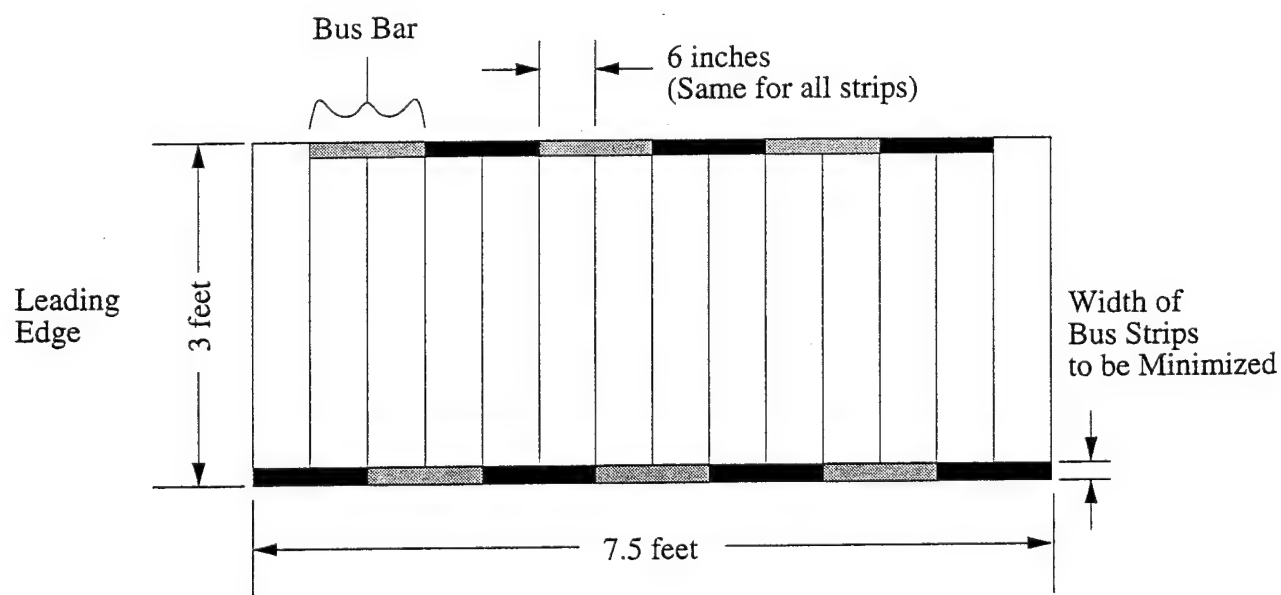


Figure 6. Layout of Monel Heating Element within the Heated Test Surface

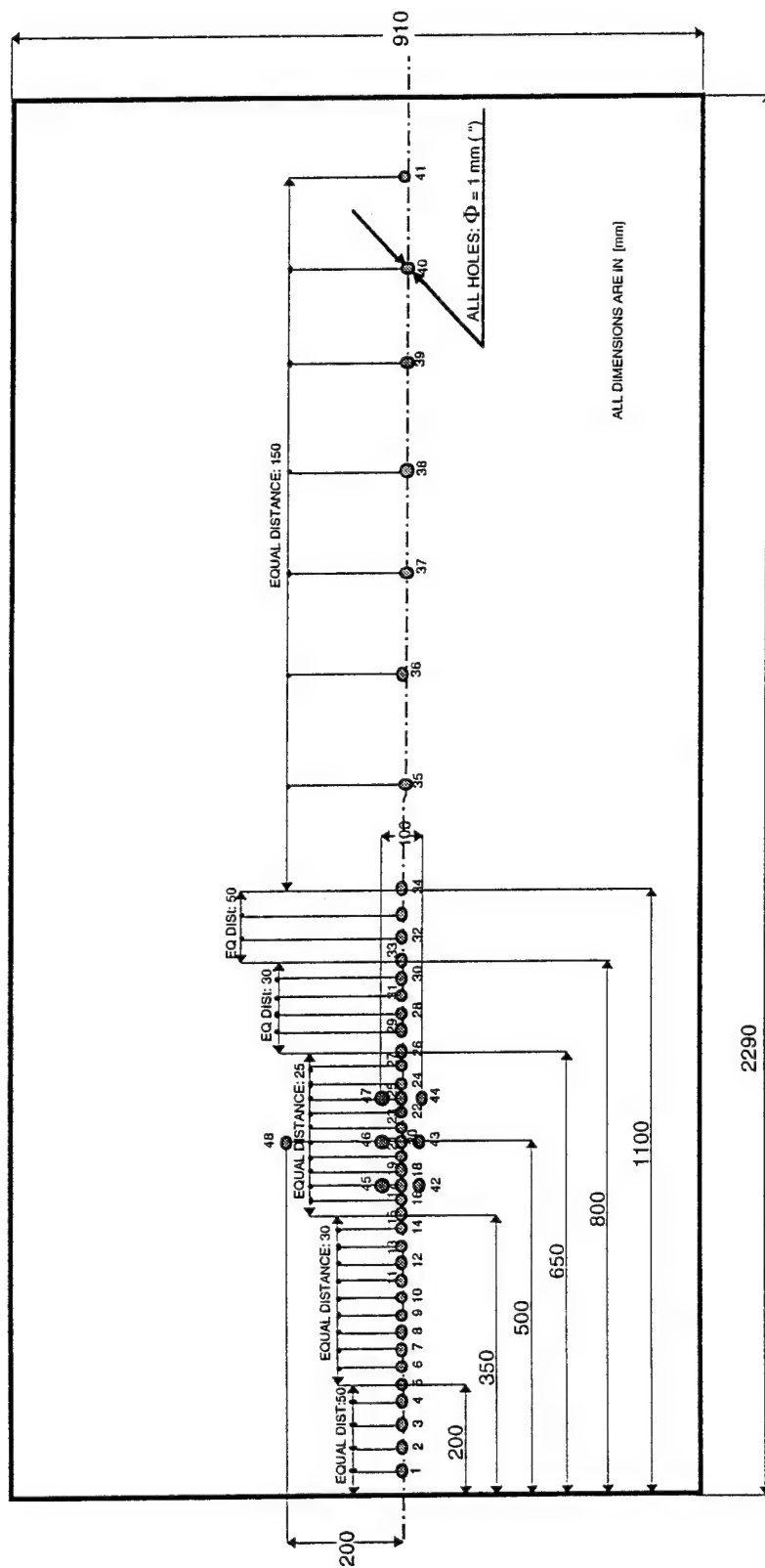
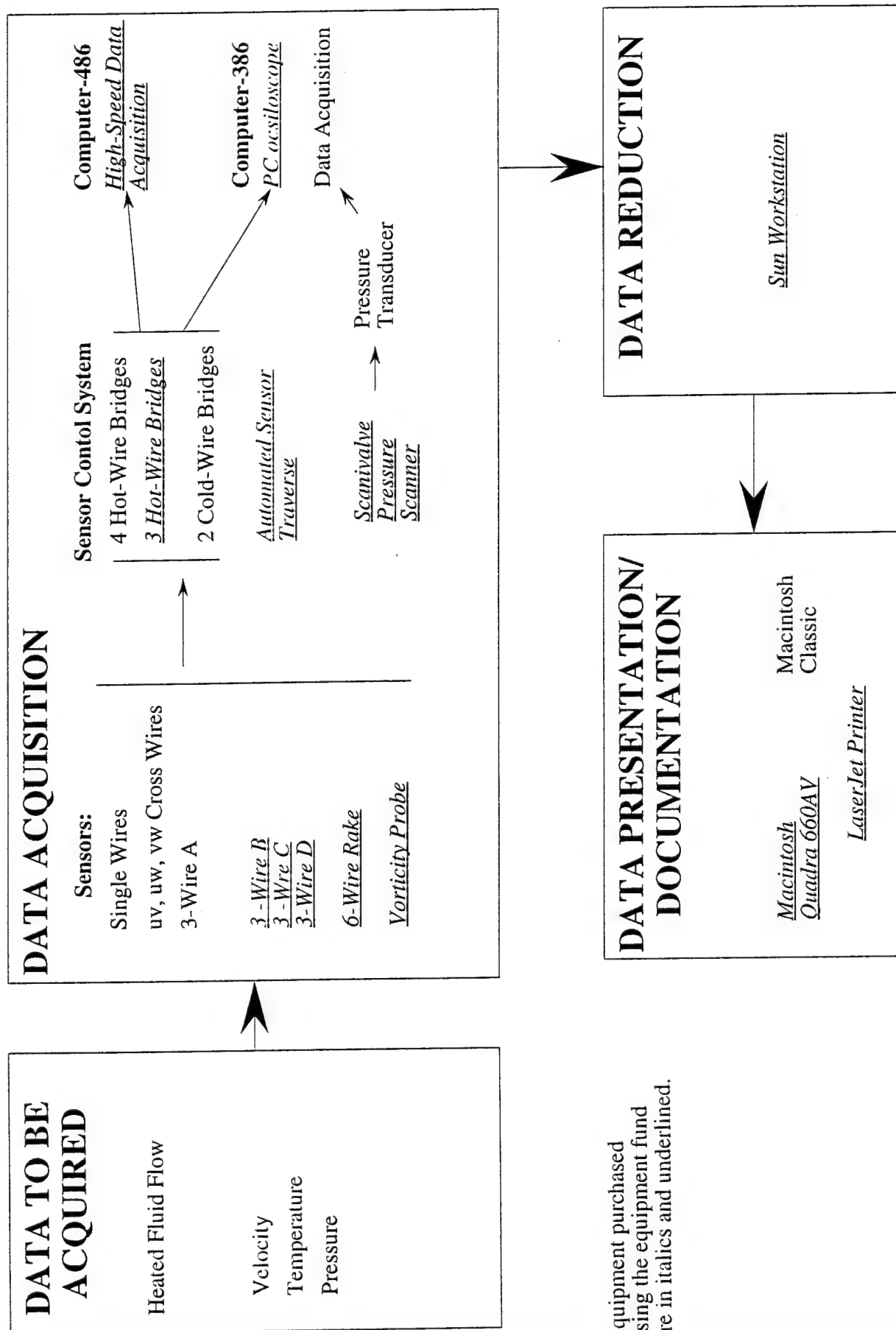


Figure 7. Layout of Static Pressure Taps on the Unheated Surface

## DATA ACQUISITION AND PROCESSING SYSTEM

The equipment fund has significantly expanded the overall experimental capabilities of the AFOSR sponsored programs at Clemson University. All of the items shown in italics in Figure 8 were purchased using this fund. The "data to be acquired" is generated using an existing wind tunnel test facility, but the test section itself, as discussed in the previous section, was constructed using the equipment fund. Every aspect of the data path has been expanded: New sensors were purchased; hardware used to position and control those sensors was obtained; new and faster machines were purchased to reduce data acquisition and reduction time; a new printer dedicated to the parent program was purchased. Every area of the AFOSR sponsored programs has benefited from this equipment grant.



Equipment purchased using the equipment fund are in italics and underlined.

Figure 8. Data Path

## PROBE DESIGNS AND PRELIMINARY RESULTS

### Probe Design

The five probes purchased using the equipment grant are shown in Figures 9 thru 13. Probes B and C shown in Figures 9 and 10 represent two variations of a three-wire sensor (Three-Wire Probe A) previously constructed using funds from the parent program. The main difference between each of the three three-wire probes is the location of the temperature sensor relative to the two velocity sensors. The temperature sensor of probe A is located to one side of the velocity sensors. In probe B, the temperature sensor is located between the velocity sensors, and in probe C it is perpendicular to and forward of the velocity sensors. The reasoning behind these design variations is presented in the next two sections.

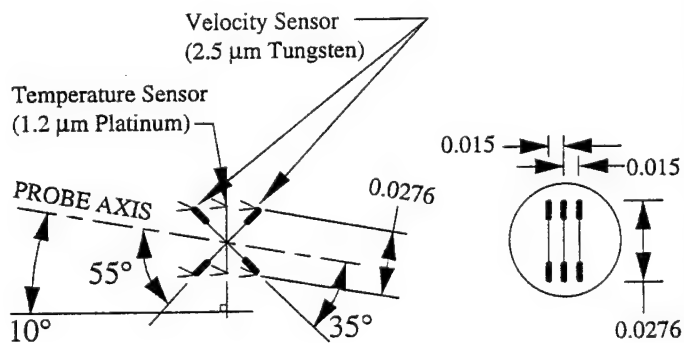
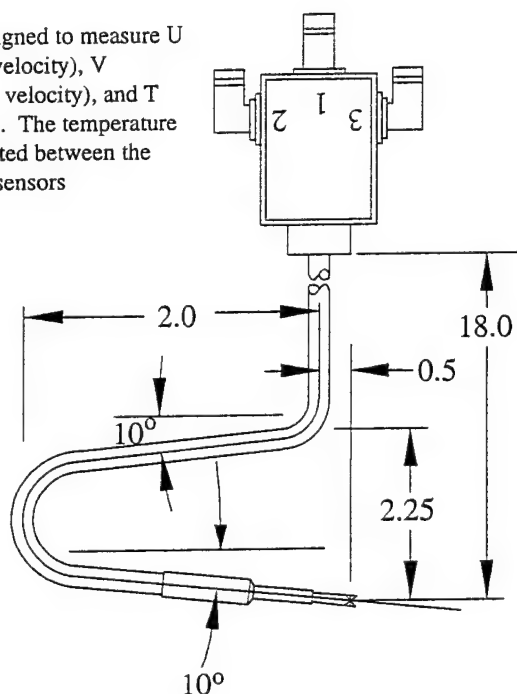
The remaining three sensors expand the measurement capabilities of the program. The three-wire probe shown in Figure 11 allows the spanwise Reynolds stress,  $\overline{uw}$ , and Reynolds heat flux,  $\overline{wt}$ , to be measured, and when used in conjunction with three-wire probe C, each of the Reynolds stresses and heat fluxes may be measured in a given flow situation (including streamwise, cross-stream, and spanwise components). In previous experiments, the data obtained from each probe was confined to a single measurement volume, but with the use of the six-wire rake shown in Figure 12, velocity measurements from six different spatial locations are possible which will allow for more detailed measurement of the spatial correlation of the instantaneous boundary layer structure. Finally, the probe shown in Figure 13 will allow measurements of vorticities and vorticity-temperature correlations,  $\overline{\omega_y t}$  and  $\overline{\omega_x t}$ , to be made within the boundary layer.

### Reynolds Heat Flux Estimation

Previously, measurements of the cross-stream Reynolds heat flux ( $\overline{vt}$ ) were made using three-wire probe A. In several previous experiments, negative values of  $\overline{vt}$  were measured in the transitional flow (Wang, Keller, and Zhou, 1992) by the probe. As stated in the previous section, the temperature sensor is located to one side of the two velocity sensors. In this situation, the distance between the temperature sensor and each of the velocity sensors is unequal. Three-wire probe B was designed to determine whether or not the negative  $\overline{vt}$  values were the result of the asymmetrical sensor distance between the hot and cold wires. The reason why the unequal separation distance is suspected of causing the negative values is because of the way  $\overline{vt}$  is experimentally calculated.



Sensor is designed to measure U (streamwise velocity), V (cross-stream velocity), and T (temperature). The temperature sensor is located between the two velocity sensors

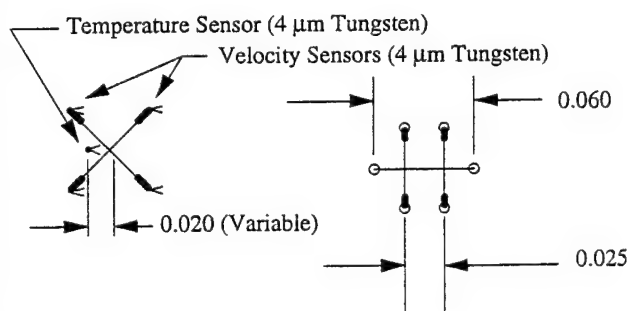
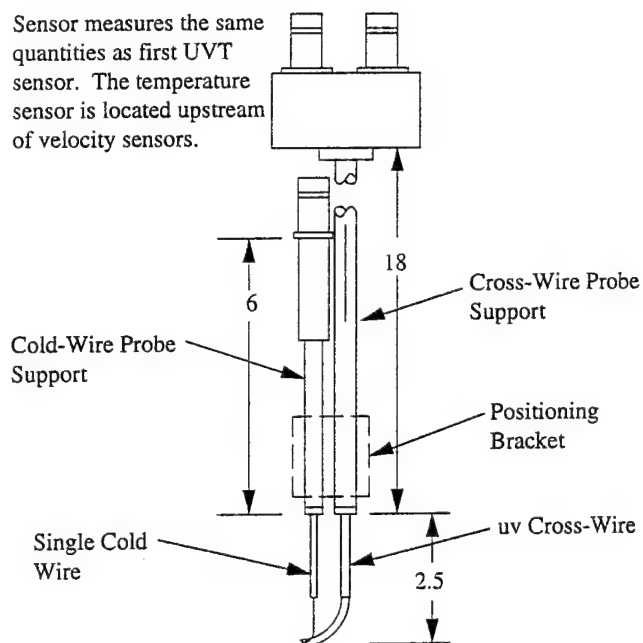


SIDE VIEW

END VIEW

Figure 9. Three-Wire Probe B

Sensor measures the same quantities as first UVT sensor. The temperature sensor is located upstream of velocity sensors.



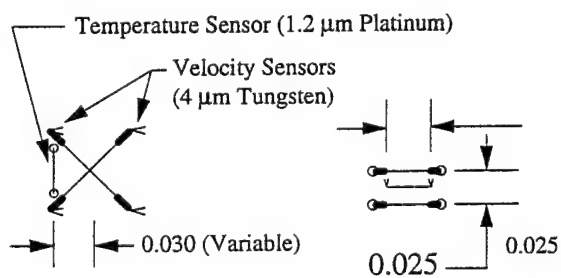
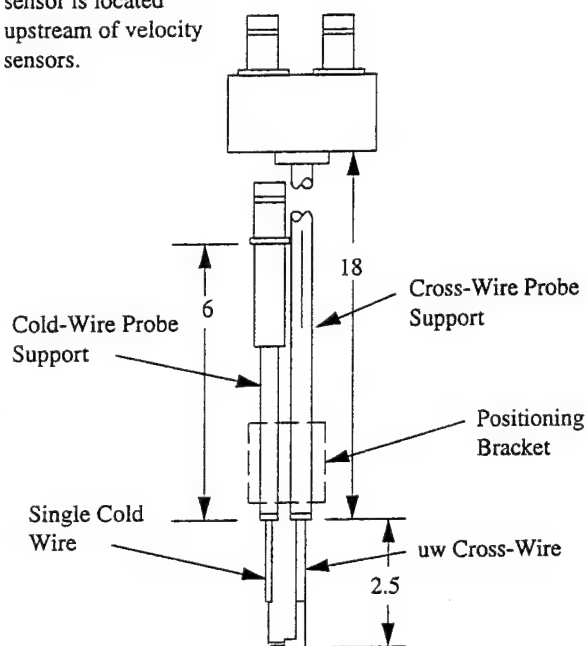
SIDE VIEW

END VIEW

Figure 10. Three-Wire Probe C

DIMENSIONS IN INCHES EXCEPT AS NOTED

Sensor measures U, W(spanwise velocity), and T. Temperature sensor is located upstream of velocity sensors.

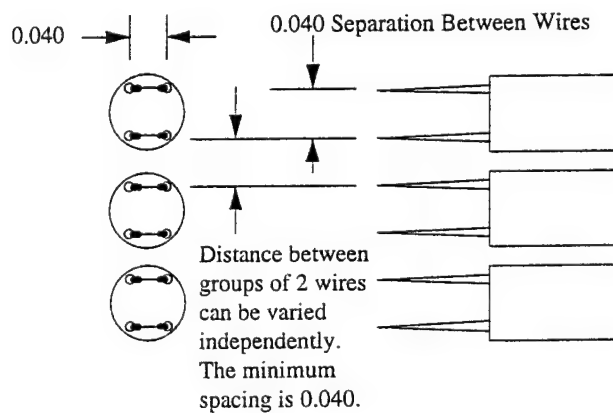
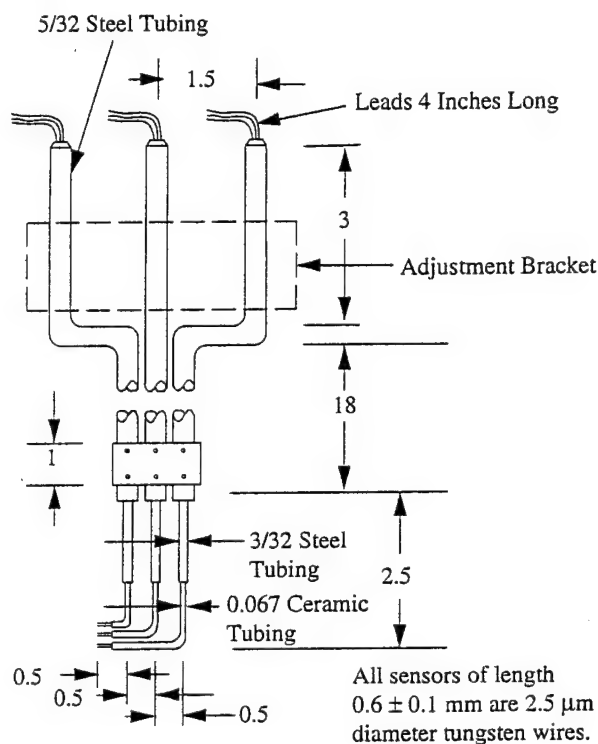


TOP VIEW

END VIEW

Figure 11. Three-Wire Probe D

Sensor array measures U at six different spatial locations simultaneously.



END VIEW

SIDE VIEW

Figure 12. Six-Wire Rake

DIMENSIONS IN INCHES EXCEPT AS NOTED

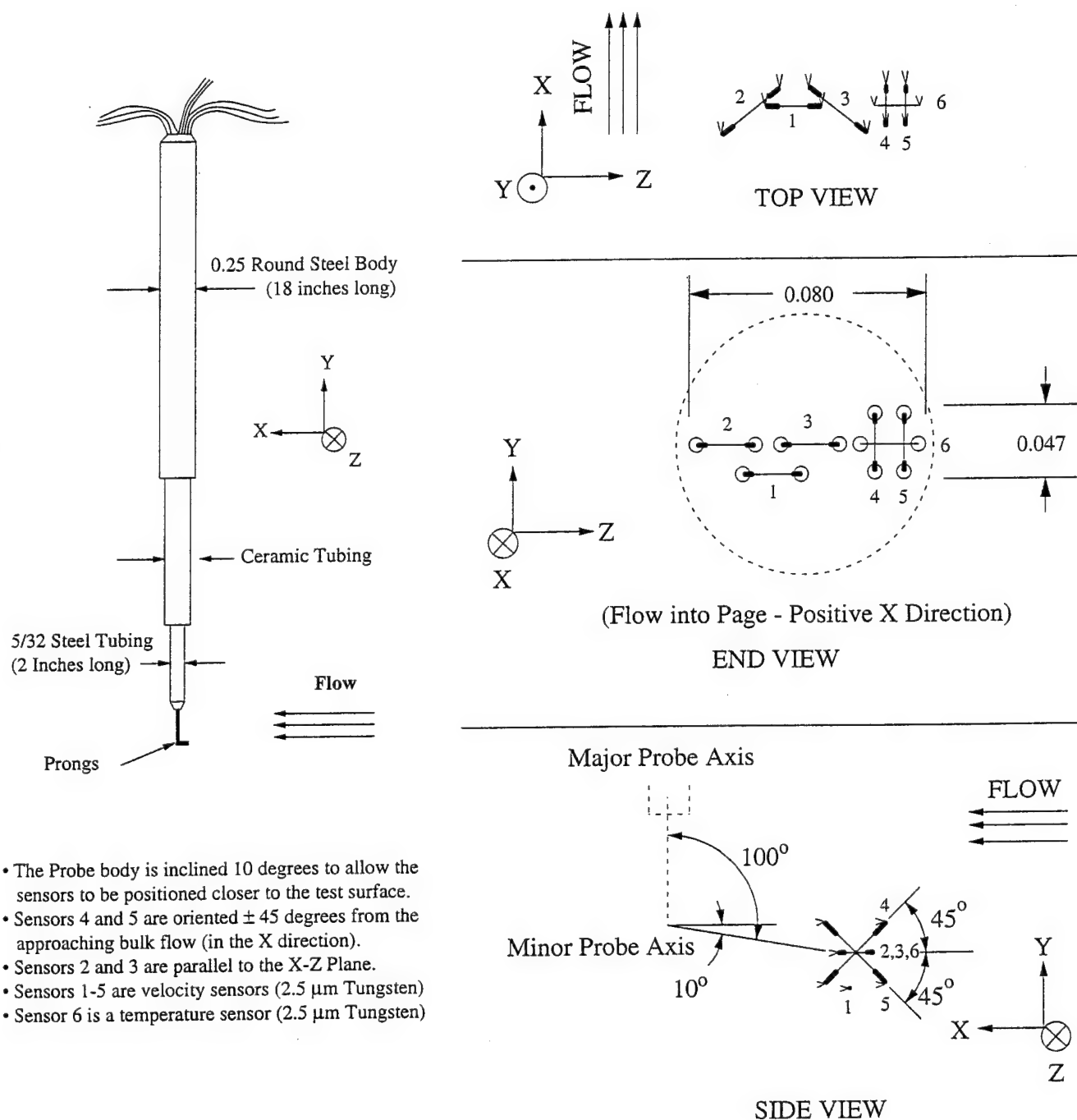


Figure 13. Vorticity and Temperature Probe

DIMENSIONS IN INCHES EXCEPT AS NOTED

Using two velocity sensors to calculate two components of velocity requires that each of the sensors be placed at a known angle with respect to the flow. Knowing the effective velocity sensed by each velocity sensor allows the two velocity components to be calculated using trigonometry. If one velocity sensor is oriented  $+45^\circ$  with respect to the streamwise bulk flow and the other is oriented at  $-45^\circ$ , then the streamwise and cross-stream velocity components may be estimated using

$$u = \frac{u_{\text{eff},1} + u_{\text{eff},2}}{\sqrt{2}} \quad \text{and} \quad [1]$$

$$v = \frac{u_{\text{eff},1} - u_{\text{eff},2}}{\sqrt{2}}, \quad [2]$$

where  $u_{\text{eff},1}$  and  $u_{\text{eff},2}$  are the effective velocities measured by each slanted wire, respectively. In the three-wire arrangement the temperature sensor is located beside the X-wire array and is presented as a function of the effective velocities, therefore  $\overline{vt}$  can be calculated using

$$\overline{vt} = \frac{\overline{u_{\text{eff},1}t} - \overline{u_{\text{eff},2}t}}{\sqrt{2}}. \quad [3]$$

If the measured  $\overline{u_{\text{eff},1}t}$  is assumed to be linearly correlated to the actual value of  $\overline{u_{\text{eff},1}t}$ , then the measured value of  $\overline{vt}$  is determined from

$$\overline{vt}_{\text{measured}} = \frac{r_1 \overline{u_{\text{eff},1}t} - r_2 \overline{u_{\text{eff},2}t}}{\sqrt{2}}, \quad [4]$$

where  $r_1$  and  $r_2$  represent the linear correlation relating the measured and actual values. Finally, if the actual effective velocities in [4] are replaced by expressions for  $u$  and  $v$  using [1] and [2], then the measured  $\overline{vt}$  is

$$\overline{vt}_{\text{measured}} = \frac{r_1 - r_2}{2} \overline{ut} + \frac{r_1 + r_2}{2} \overline{vt}. \quad [5]$$

If the correlation values  $r_1$  and  $r_2$  are not equal, then the measured value for the cross-stream Reynolds heat flux becomes a function of both the cross-stream and the streamwise components. Since  $\overline{ut}$  is significantly higher (at least one order of magnitude) than  $\overline{vt}$  in the transitional and turbulent portions of a boundary layer, it is possible that even small discrepancies between  $r_1$  and  $r_2$  could introduce a fictitious value of the first term in equation [5]. This fictitious term can be in the same order of magnitude of the second term and can create negative values in the calculated  $\overline{vt}$ . Given the small eddy sizes present during transition and turbulence, it seems likely that  $r_1$  and  $r_2$  are different for three-wire probe A because the distance between velocity sensor 1 is twice as far away from the temperature sensor as is velocity sensor 2. It was then speculated that the unequal distance between the hot and

cold wires was the most probable cause of negative  $\overline{v_t}$  in the transitional boundary layer.

To remedy this situation, three-wire probe B was designed with the temperature sensor located between the two velocity sensors. Once the probe was received and calibrated, the cross-stream Reynolds heat flux was measured using three-wire probes A and B in the transitional and turbulent portions of a boundary layer over a heated test surface. The cross-stream variation in  $\overline{v_t}$ , normalized by the wall heat flux, for each probe in the transitional portion of the boundary layer is shown in Figure 14. Similarly, Figure 15 shows the variation in the fully turbulent portion of the boundary layer. In both figures, three-wire probe A measures negative values as low as -0.1 for  $y/\delta$  less than 0.1. Conversely, three-wire probe B measures  $\overline{v_t}$  between 0.17 to 0.2 in the same region of the boundary layer under the same conditions. These results suggest that our speculation regarding the symmetric hot-cold wire arrangement as the culprit of the negative  $\overline{v_t}$  is correct. For accurate  $\overline{v_t}$  measurements, the temperature sensor must be equidistant from each of the velocity sensors.

#### X-Wire Spacing Analysis

As stated in the previous section, the design of three-wire probe B called for the temperature sensor to be placed between the velocity sensors. Due to construction constraints imposed by TSI Incorporated, the manufacturer of probe B, the spacing between the two velocity sensors was 1.07 mm. This distance is twice as large as the velocity sensor spacing on three-wire probe A. During testing of three-wire probes A and B, significant differences in measured values of the cross-stream Reynolds stress,  $\overline{uv}$ , were observed; therefore, a more detailed investigation of the effects of velocity sensor spacing was deemed necessary.

As before, the flow condition used for testing was the boundary layer over a flat plate, but this time the surface was not heated to reduce effects of thermal transport within the flow. A total of five streamwise locations representing various stages of laminar, transition, and turbulent flow regimes were selected for cross-stream measurements using four sensors: a single wire (TSI model 1218-T1.5), a standard u-v cross-wire (TSI model 1243-T1.5, sensor spacing 1.17 mm), a modified u-v cross-wire (part of three-wire probe C, sensor spacing 0.79 mm), and three-wire probe B. The results of the single hot wire analysis shown in Figure 16 indicate that laminar-turbulent transition occurred between a Reynolds number of  $5.28 \times 10^5$  and  $9.76 \times 10^5$ . The curved lines represent the Blasius solution for flow over a flat plate and the turbulent correlation, respectively. Subsequent comparisons of the measured Reynolds normal and shear stresses will involve the latter four streamwise locations documented in Figure 16.

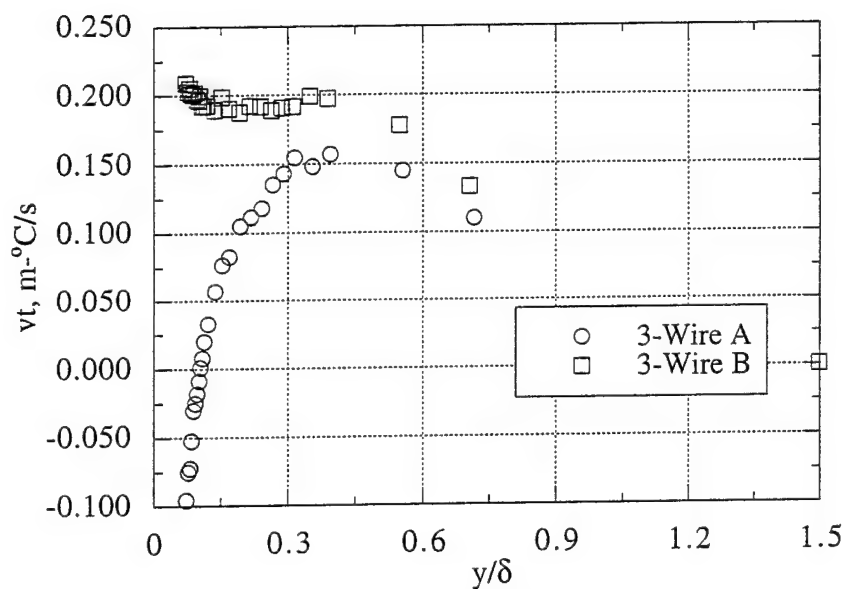


Figure 14. Cross-Stream Reynolds Heat Flux Comparison: Late Transition

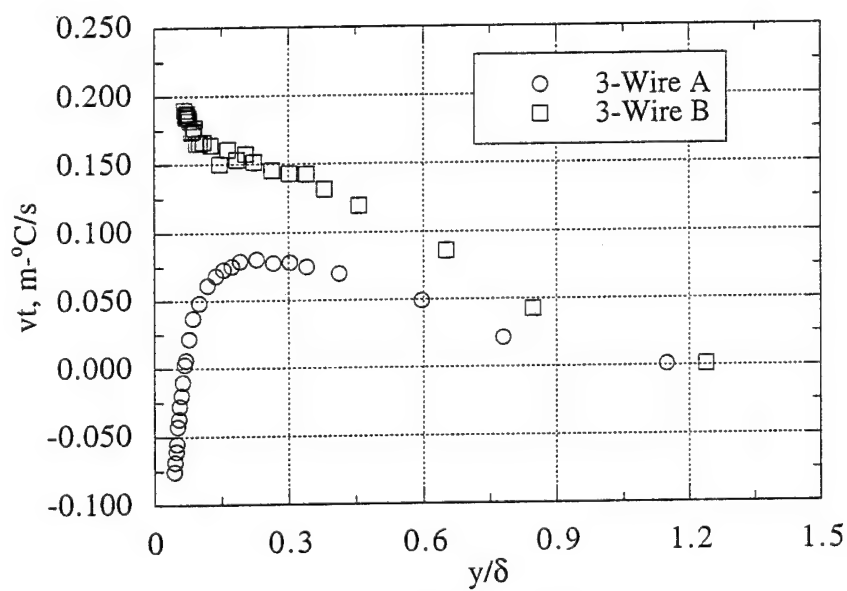


Figure 15. Cross-Stream Reynolds Heat Flux Comparison: Early Turbulent Flow

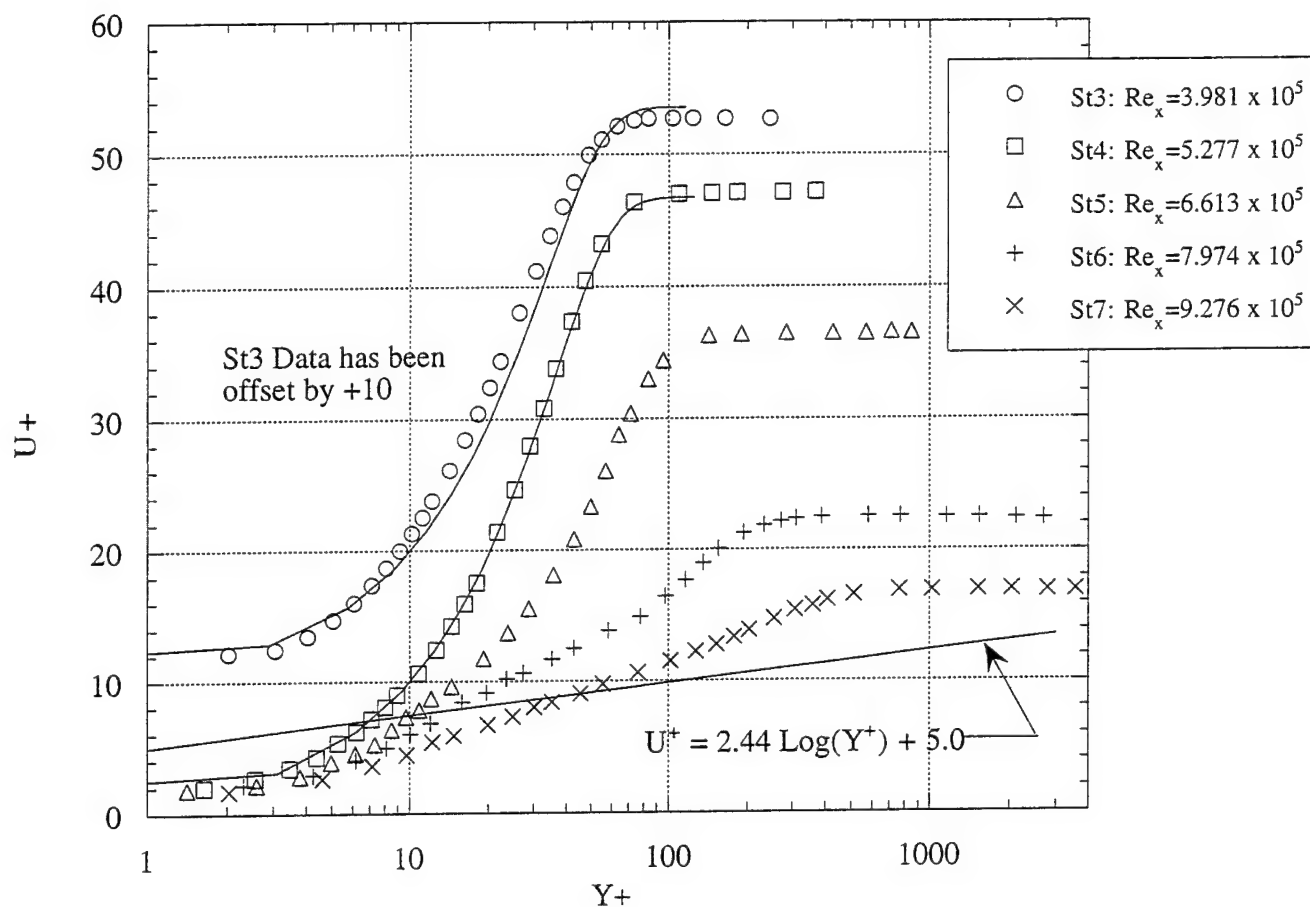


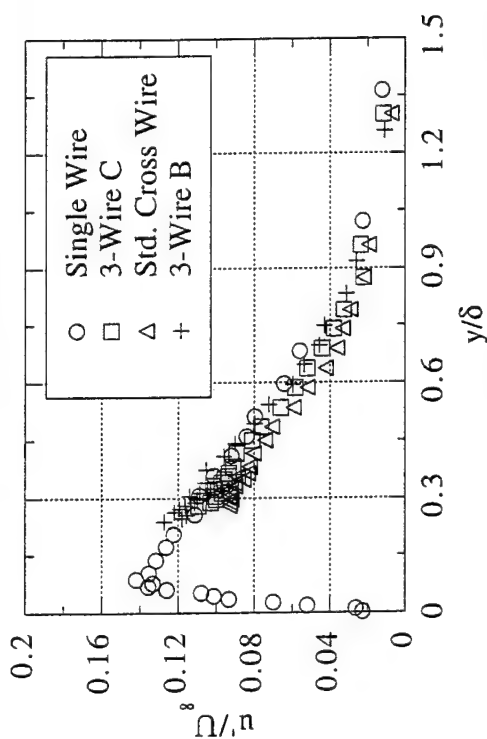
Figure 16. Normalized Single Hot Wire Data

The measured values for Reynolds streamwise normal stress,  $u'$ , are shown in Figure 17. Overall, the agreement among the sensors was good. The largest scatter was observed in the late laminar and the early transitional measurements (Figures 17a and 17b, respectively). Between  $0.25$  and  $0.5 y/\delta$ , the scatter was approximately 25%. In the case of the cross-stream Reynolds stress,  $v'$ , the scatter in the same region of the boundary layer ( $0.25 < y/\delta < 0.5$ ) was also approximately 25%, but in this case the scatter was of this order of magnitude in the laminar, transitional, and turbulent portions of the boundary layer as shown in Figure 18. Measurements shown in Figures 18a, 18b, and 18c show that three-wire probe C gives the lowest measurements and that three-wire B gives the highest ones; however, the standard cross-wire gives distinctly higher measurements in the turbulent boundary layer, as shown in Figure 18d. Measurements of the cross-stream Reynolds shear stress,  $\overline{uv}$ , are shown in Figure 19. In all cases, but particularly the early transitional case of Figure 19b, three-wire B gives significantly higher measurements than either the standard cross-wire or three-wire C. Generally, the standard cross-wire and three-wire C are within 35% of each other, but the measurements of three-wire B are 30% to 100% higher than those of the other sensors.

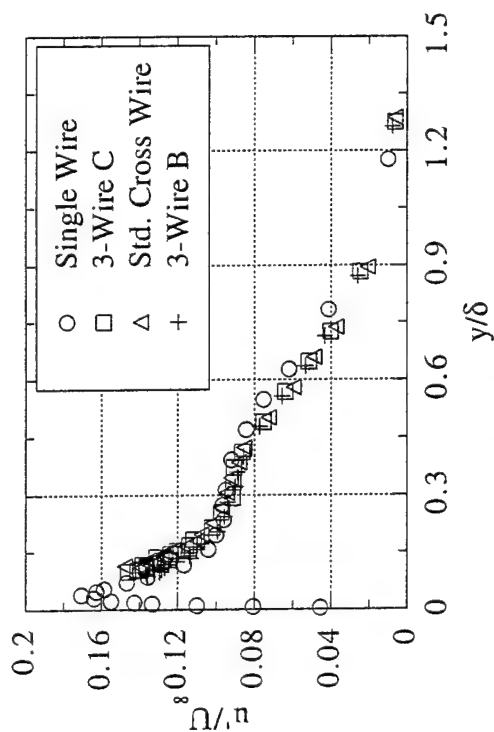
The correlation coefficient between the effective velocities of each probe is shown in Figure 20. The effective velocities were used rather than  $u$  and  $v$  because the effective velocities both contain a component of  $u$ , the dominant velocity component, and as a result the correlation between the effective velocities gives a coefficient more representative of the statistical similarity of the flow as sensed by the two sensors (looking at the correlation coefficient between  $u$  and  $v$  would have given indications more significant to a description of the flow isotropy than of the similarities between the flow conditions sensed by the wires). Figure 20a shows that for 75% of the boundary layer, all three sensors show a correlation greater than 0.95 in the laminar portion of the boundary layer. The correlation for three-wire probe B decreases before those of either of the other two probes. The situation for the fully turbulent boundary layer is shown in Figure 20b. Over the same region of the boundary layer, the overall correlation has decreased to about 0.75, but again the correlation for three-wire probe B is lower than those of the other probes. In the case shown, the correlation for three-wire probe B is 9% less than the correlation of the standard cross-wire and three-wire probe C.

The above results imply that three-wire probe B resolves the controversial negative  $\overline{vt}$  problem; however, it introduces wire spacing problems. The discrepancy of  $\overline{uv}$  measurement between the standard cross-wire and three-wire probe B is speculated to be caused by the flow disturbances generated by the cold wire, which is situated between the two hot-wire velocity sensors.

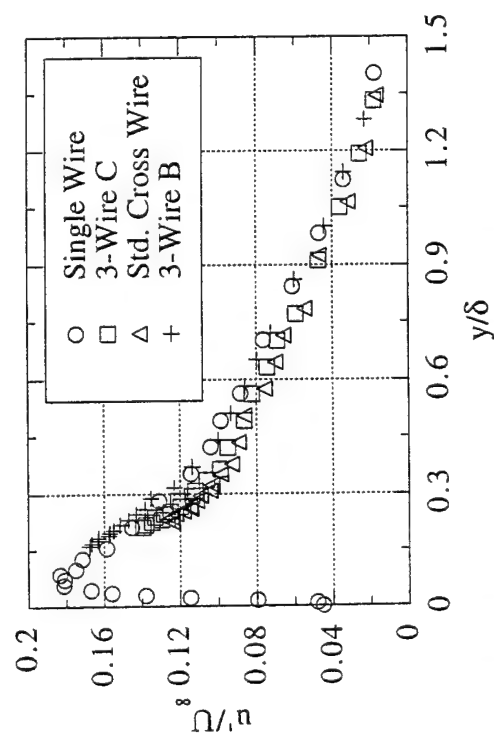




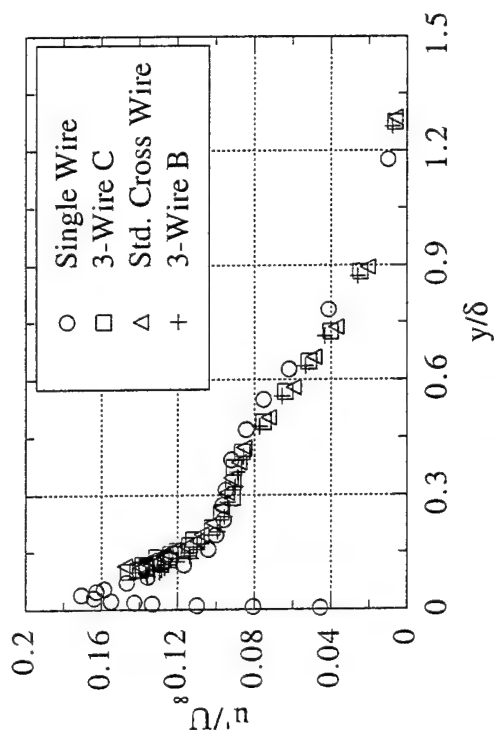
(a) Laminar Boundary Layer:  $Re_x = 5.277 \times 10^5$



(b) Early Transitional Boundary Layer:  $Re_x = 6.613 \times 10^5$

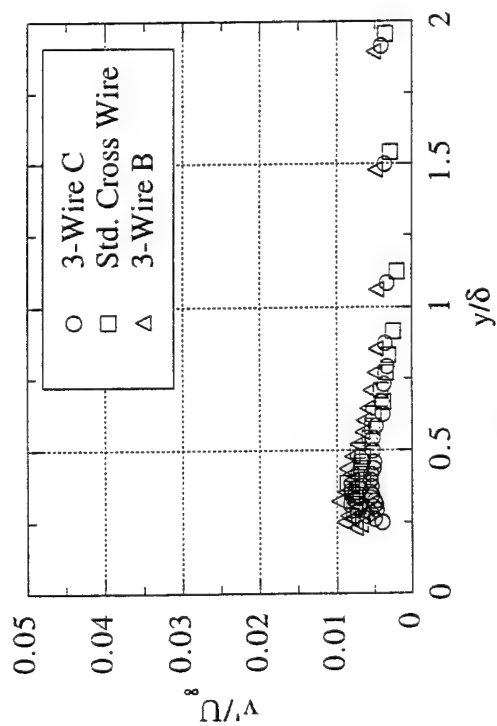


(c) Late Transitional Boundary Layer:  $Re_x = 7.974 \times 10^5$

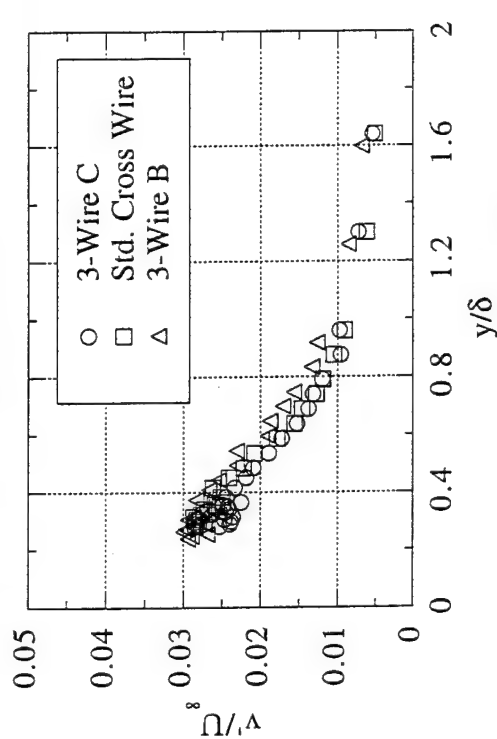


(d) Early Turbulent Boundary Layer:  $Re_x = 9.276 \times 10^5$

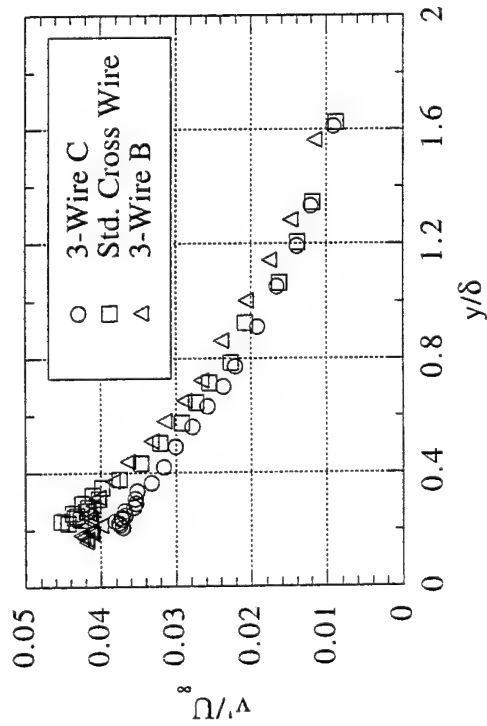
Figure 17. Streamwise Reynolds Normal Stress Comparison



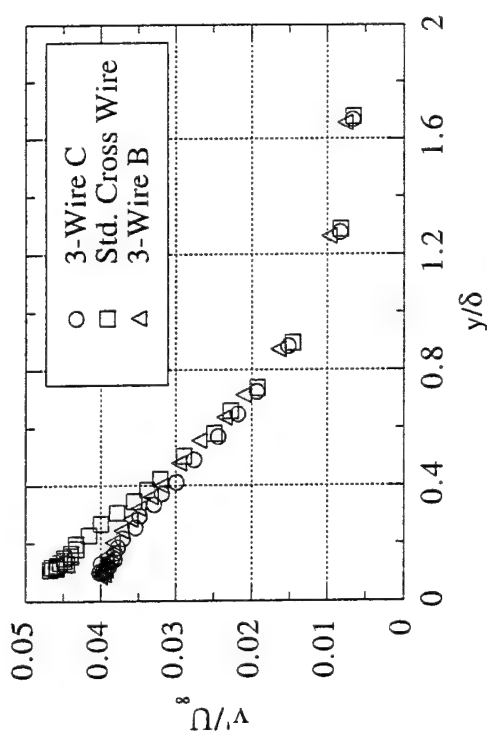
(a) Laminar Boundary Layer:  $Re_x = 5.277 \times 10^5$



(b) Early Transitional Boundary Layer:  $Re_x = 6.613 \times 10^5$

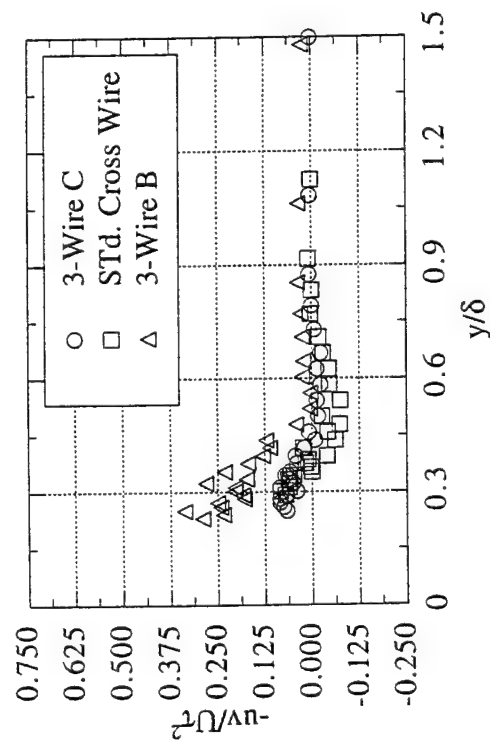


(c) Late Transitional Boundary Layer:  $Re_x = 7.974 \times 10^5$

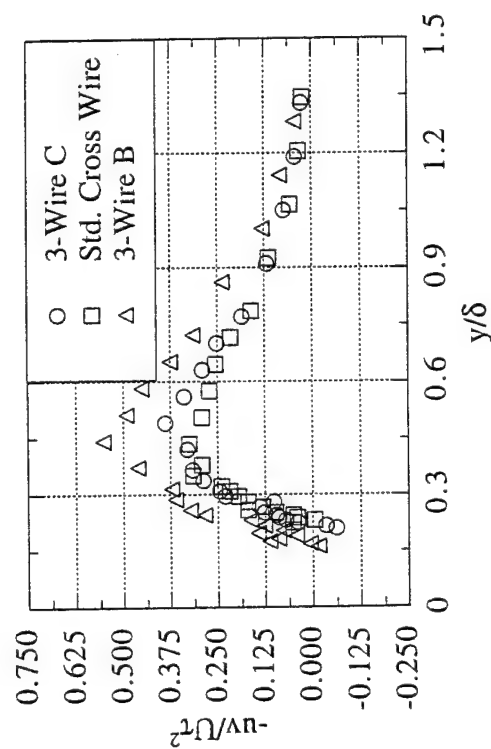


(d) Early Turbulent Boundary Layer:  $Re_x = 9.276 \times 10^5$

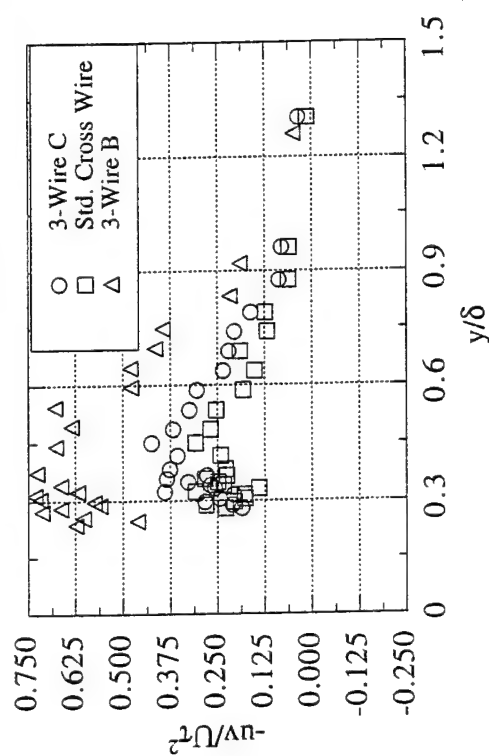
Figure 18. Cross-Stream Reynolds Normal Stress Comparison



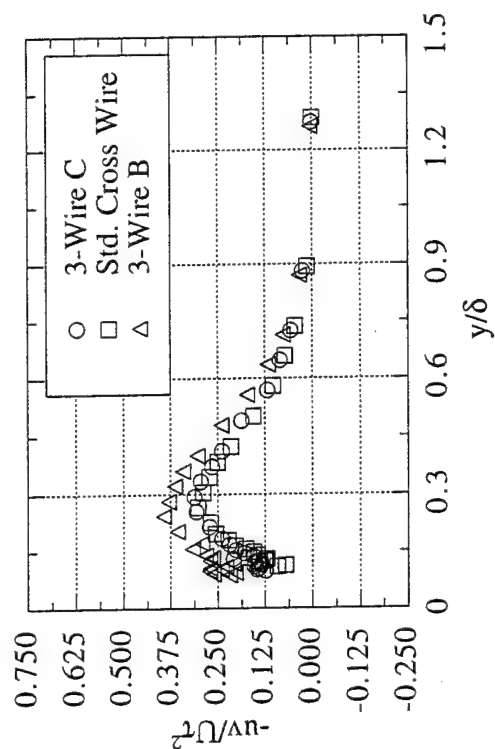
(a) Laminar Boundary Layer:  $Re_x = 5.277 \times 10^5$



(c) Late Transitional Boundary Layer:  $Re_x = 7.974 \times 10^5$

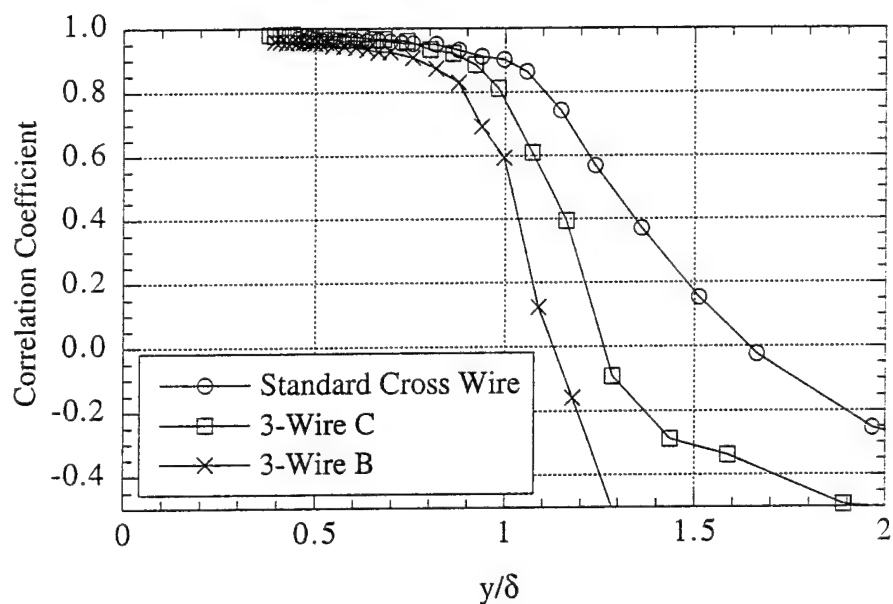


(b) Early Transitional Boundary Layer:  $Re_x = 6.613 \times 10^5$

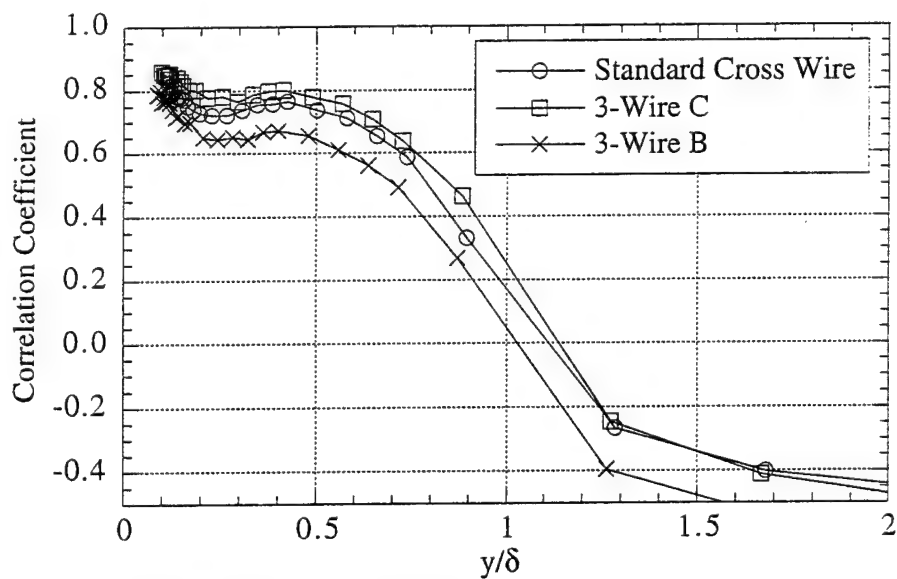


(d) Early Turbulent Boundary Layer:  $Re_x = 9.276 \times 10^5$

Figure 19. Cross-Stream Reynolds Shear Stress Comparison



(a) Laminar Boundary Layer:  $Re_x = 5.277 \times 10^5$



(b) Early Turbulent Boundary Layer:  $Re_x = 9.276 \times 10^5$

Figure 20. Comparison of Correlation Coefficient

## Conclusions

1. The cold wire should be placed equidistant from the hot wires for proper  $\overline{v_t}$  estimation.
2. The spacing of the hot wires in the standard cross wire and three-wire probe B is about the same (1.17 mm and 1.07 mm, respectively), but the large discrepancy in  $\overline{uv}$  measurements in the transitional portion of the boundary layer suggests that the cold wire should not be located between the hot wires. The change in correlation between the hot wires with separation distance suggests that the spacing should be as close as possible.

As a result of the above observations, three-wire probe C was designed to incorporate both tight spacing and symmetric layout between the hot and cold wires. For probe C the cross-wire spacing is 0.79 mm, and the temperature sensor is placed slightly forward of and perpendicular to the plane of the hot wires. In this way, the temperature sensor can be equidistant of the hot wires, but the temperature sensor is not between the hot wires so that the hot-wires can be spaced more closely together.

## References

Wang, T., Keller, F.J., and Zhou D., "Experimental Investigation of Reynolds Shear Stresses and Heat Fluxes in a Transitional Boundary Layer," ASME paper, HTD Vol. 226: Fundamental and Applied Heat Transfer Research for Gas Turbine Engines, pp. 61-70.

## CURRENT STATUS

Except for the items listed below, all equipment has been received and is fully operational.

1. The cross-wire portion of 3-wire probe C has been tested, but testing of the temperature sensor in conjunction with the cross-wire has not been completed.
2. Three-wire probe D has been received, but it has not been tested.
3. The vorticity probe and the 6-wire rake were received 4 December 1995, and they have not been tested yet.
4. The new test section is still under construction, but it is almost complete. The adhesive holding the heated test surface to the Lexan support sheet needs to be improved before testing can be initiated.

## PUBLICATIONS

The work of the following published papers was completed by using the facility and equipment supported by this equipment grant:

Journal Papers

Wang, T. and Zhou, D., "Spectral Analysis of Transitional Boundary Layer on a Heated Plate," accepted for publication in the International Journal of Heat and Fluid Flow, July 1995.

Mislevy, S. P. and Wang, T., "The Effects of Adverse Pressure Gradients on Momentum and Thermal Structures in Transitional Boundary Layers. Part 1: Mean Quantities," accepted for publication in ASME Journal of Turbomachinery, 1995

Mislevy, S. P. and Wang, T., "The Effects of Adverse Pressure Gradients on Momentum and Thermal Structures in Transitional Boundary Layers. Part 2: Fluctuation Quantities," accepted for publication in ASME Journal of Turbomachinery, 1995

Wang, T., J. F. Keller, and Zhou, D. D., "Experimental Investigation of Reynolds Shear Stresses and Heat Fluxes in a Transitional Boundary Layer," Accepted for publication in the Journal of Experimental Fluid and Thermal Science, July 1995.

Zhou, D. and Wang, T., "Combined Effects of Elevated Free-Stream Turbulence and Streamwise Acceleration on Flow and Thermal Structures in Transitional Boundary Layers," accepted for publication in the Journal of Experimental Fluid and Thermal Science, July 1995.

Keller, F. J. and Wang, T., "Flow and Heat Transfer Behavior in Transitional Boundary Layers with Streamwise Acceleration," accepted for publication at the ASME Journal of Turbomachinery, 1995

Zhou, D. D. and Wang, T., "Laminar Boundary Layer Flow and Heat Transfer with Favorable Pressure Gradient at Constant K Values," submitted to the International Journal of Heat and Mass Transfer, 1995.

Keller, F. J. and Wang, T., "Effects of Criterion Functions on Intermittency in Heated Transitional Boundary Layers with and without Streamwise Acceleration," ASME Journal of Turbomachinery, Vol 117, No. 1, pp. 154-165, 1995.

Zhou, D. and Wang, T., "Effects of Elevated Free-stream Turbulence on Flow and Thermal Structures in Transitional Boundary Layers," ASME Journal of Turbomachinery, Vol. 117, No.3, pp.407-417, 1995.

Conference Papers

Wang, T. and Zhou, D., "Spectral Analysis of Transitional Boundary Layer on a Heated Plate," Presented at the Sixth Asian Congress of Fluid Mechanics, Singapore, May 1995.

Mislevy, S. P. and Wang, T., "The Effects of Adverse Pressure Gradients on Momentum and Thermal Structures in Transitional Boundary Layers. Part 1: Mean Quantities," ASME paper 95-GT-4, presented at the 1995 ASME International Gas Turbine Congress, Houston, June, 1995.

Mislevy, S. P. and Wang, T., "The Effects of Adverse Pressure Gradients on Momentum and Thermal Structures in Transitional Boundary Layers. Part 2: Fluctuation Quantities," ASME paper 95-GT-5, presented at the 1995 ASME International Gas Turbine Congress, Houston, June, 1995.

Cai, Y., Wang, T. and Golan, L.P., "Mixed Convection of Heat and Moisture in the Crawl Space of Manufactured Housing," 1995 National Heat Transfer Conference Proceedings, Vol. 8 (or ASME HTD-Vol.310), pp.139-148, 1995

Keller, F. J. and Wang, T., "Flow and Heat Transfer Behavior in Transitional Boundary Layers with Streamwise Acceleration," ASME Paper 94-GT-24, Presented at the 1994 International Gas Turbine Congress, Netherlands, June 1994.

Pinson, M. and Wang, T., "Effects of Leading Edge Roughness on Flow and Heat Transfer in Transitional Boundary Layers," ASME Paper 94-GT-326, Presented at the 1994 International Gas Turbine Congress, Netherlands, June 1994.

Wang, T., Cai, Y., and Golan, L. P., "Heat and Moisture Transfer in an Enclosure -- With an Application to the Crawl Space of Manufactured Housing with Forced Ventilation," to be submitted to a conference in, 1994.

Zhou, D. and Wang, T., "Combined Effects of Elevated Free-Stream Turbulence and Streamwise Acceleration on Flow and Thermal Structures in Transitional Boundary Layers," in Gas Turbine Heat Transfer, ASME HTD-Vol. 242, pp. 41-53, presented at the 1993 National Heat Transfer Conference, August 1993, Atlanta, GA.

#### PERSONNEL

The following students have been benefited from using the facility and equipment supported by this equipment grant:

F. Jeffery Keller (Ph. D)  
Anca Hatman (Ph.D)

Dadong Zhou (Ph. D)  
Mark W. Pinson (Ph.D)

Scott P. Mislevy (M.S)



# College of Engineering

DEPARTMENT OF MECHANICAL ENGINEERING



October 18, 1994

Ms. M. McKee  
Contracting Officer  
AFOSR /PKA  
110 Duncan Avenue  
Bolling AFB, DC 20332-0001

Subject: No-Cost Extension for Grant No. F49620-93-1-0533

Dear Ms. McKee:

On August 15, 1994 I submitted a request to extend Grant No. F49620-93-1-0533 from 9/28/94 to 9/28/95 at no additional cost. A budget was proposed for the remaining funds in that request. However, due to the changing experimental conditions, the project's priorities have also changed. The following explanations give the reasons for delaying the purchase of two originally budgeted sensors and for acquiring new priority items at no additional cost.

1. Explanation for delaying the purchase of sensors B and C --- The final designs of sensors B and C depend on the test results of sensor A. Due to the difficulty of fabricating sensor A, the manufacturer (TSI Inc.) delayed the delivery of Sensor A until mid-July, 1994. Since the quality and survivability of Sensor A has not been completely qualified, the final design and ordering of sensors B and C has been subsequently delayed. In addition, due to the difficulty involved in fabricating Sensor A, the manufacturer has notified us that the price quoted in 1993 for sensors B and C will be increased. However, the increased price can be absorbed by the existing budget due to reduced costs for other items.
2. Justification for replacing the test surface, the test section, and the associated powering system --- About two weeks ago, our heated test wall started to show unsatisfactory aging symptoms, possibly due to cyclic heating and cooling during the last four years. The test wall is the soul of our experiments; without a satisfactory test wall, the proposed delicate sensors, updated data acquisition apparatus, and enhanced data processing capabilities will be of no use. This test rig has been used by two other projects which are supported by an EPSCOR fellowship grant (No. F49620-92-J-0459)

and an AFOSR grant (No. F49620-94-0126). Unless the test wall is replaced, all three of the projects will be adversely affected.

3. Justification for purchasing a 24-channel scanivalve system --- The pressure measurements have been performed manually by plugging and unplugging the tubes which connect to the pressure taps. This is a labor-intensive and time-consuming process. To increase the efficiency of conducting pressure measurements, an automatic pressure-scanning system is required. This can reduce the time required for one round of pressure measurements from 30 minutes to within one minute.

The attached revised budget for the requested extension period is based on my best judgement of how to most effectively use the remaining grant money to purchase the most appropriate and needed equipment to perform the ongoing research programs. In view of the urgency and seriousness of replacing the old test wall and associated powering system with a new design, your earliest response to this request is greatly appreciated.

Sincerely yours,



Ting Wang  
Professor

cc: Mr. W. C. Hallums, Jr. (Sponsored Programs)  
Ms. Roberta Elrod (College of Engineering)  
Dr. James M. McMichael (Program Monitor)

(Revised 10/18/94)

**Revised Budget for the One Year, No-Cost Extension (9/29/94 - 9/28/95)**

**Grant No. F49620-93-1-0533**

|   |        |
|---|--------|
| Heated test surface, test section, and associated powering system | 11,000 |
| 24-channel scanivalve system                                      | 5,000  |
| Sensor B and accessories  | 5,700  |
| Sensor C and accessories  | 13,800 |
| <hr/>   |        |
| Total   | 35,500 |



DEPARTMENT OF THE AIR FORCE  
AIR FORCE OFFICE OF SCIENTIFIC RESEARCH (AFMOS)  
BOLLING AIR FORCE BASE, DC 20332-0001

AFOSR/PKA  
110 Duncan Avenue, Suite 8115  
Bolling AFB DC 20332-0001

5 January 1995

Clemson University  
Attn: Ms. Valerie Ramsay  
Office of Sponsored Programs  
Clemson SC 29634-5353

Reference is made to Professor Wang's letter, 18 October 1994. We have no objection to the reallocation of funds of grant F49620-93-1-0533 in order to purchase the requested equipment. A grant amendment adding this equipment to the grant shall be forthcoming. Should you have any questions concerning this request, please contact Ms. Jennifer Bell at (202) 767-6836.

Sincerely,

VERNITA J. SLATER  
Administrative Contracting Officer

PM/Dr. J. McMichael  
PI/Professor T. Wang